

# Signal to Noise Ratio Maximization in Quiet Zone Acquisitions for Range Assessment at Sub-millimeter Wavelengths

Alfonso MUÑOZ-ACEVEDO, Manuel SIERRA-CASTAÑER

Radiation Group, Technical University of Madrid, Av. Complutense 30, Madrid, Spain

alfonso@gr.ssr.upm.es, mscastaner@gr.ssr.upm.es

**Abstract.** *This paper proposes a quiet zone probing approach which deals with low dynamic range quiet zone acquisitions. Lack of dynamic range is a feature of millimeter and sub-millimeter wavelength technologies. It is consequence of the gradually smaller power generated by the instrumentation, that follows a  $f^\alpha$  law with frequency, being  $\alpha \geq 1$  variable depending on the signal source's technology. The proposed approach is based on an optimal data reduction scenario which redounds in a maximum signal to noise ratio increase for the signal pattern, with minimum information losses. After theoretical formulation, practical applications of the technique are proposed.*

## Keywords

Sub-millimeter wavelengths, signal to noise ratio, antenna measurements, compact antenna test range, range assessment.

## 1. Introduction

Compact Antenna Test Ranges (CATRs) are antenna measurement facilities [1] which feature the inherent advantages of farfield test techniques while keeping the size of a nearfield chamber. This compactness requires electromagnetic field collimating optics that are able to handle the radiation pattern of the feed antenna so it is transformed into a plane wave distribution, existing within a volumetric region called "quiet zone".

Diverse elements of the facility contribute to the discrepancy between the ideal case where the quiet zone is a locally plane wave distribution and the existing fields, in reality. In well designed CATRs, the main component of the quiet zone fields results from the collimation of the feeder's emerging spherical wave towards the optics. While other spurious scattering sources may affect this collimated wave thus degrading the planarity of the quiet zone, the collimated wave itself relies on the performance of the optics. At lowest frequencies, the collimating capabilities of the optics are decreased because the field scatter-

ers involved in the collimation process reduce their authority over the propagating waves [2], as a consequence of its diminished electrical size. On the other hand, at highest frequencies the mechanical accuracies in the alignment of the optics [3] and the smoothness of their surfaces become critical and accordingly set bounds to the highest frequency at which the optics collimate the fields according to certain planarity criteria, expressed in terms of rms ripples both in magnitude and phase.

Therefore, evaluation of the optics' performance constitutes the mainstream for the assessment of a CATR. It sets realistic limits to its best achievable quiet zone performance besides the interference of extraneous disturbing sources, such as radiation absorbing material or signal's multiple reflection patterns. The study can be performed at different levels: either theoretically with EM simulations of a virtual facility [4] or experimentally, performing quiet zone probing of an existing facility [5], [6]. While the first approach allows the flexible introduction of modifications in the facility so its behavior can be known in several scenarios (thus driving the conclusions extraction and eventually, optimization), [3] it always relies on simplifying hypothesis required for any algorithm [4], in addition with the fact that no matter how complete the simulation is, the calculations are not performed on the facility which actually exists. The quiet zone probing approach proves to be a powerful tool to get a clear idea of a range's performance. When the probing process is performed in 2D scans (either Cartesian or polar), with several configurations of the feed / probe antennas and for different frequencies of interest, it is able to offer a very clear image of the quiet zone's behavior. Both vector as well as complex information is then extracted so cross-polar levels are known and the collimation capabilities are clearly described.

At millimeter and sub-millimeter wavelength frequencies, the use of quiet zone probing is seriously compromised by the time consumption resulting from the  $\propto f^2$  increasing required number of samples. Moreover, the dynamic range figure offered by the instrumentation decreases  $\propto f^{-\alpha}$  with  $\alpha \geq 1$  when moving towards the sub-millimeter wavelength frequencies. Whenever SNR wants to be kept, a respective  $\propto f^{-\alpha}$  decrease in the receiver's

intermediate frequency bandwidth (IFBW) is mandatory thus increasing the acquisition time per sample  $\propto f^{+\alpha}$ . In sum, a  $\propto f^{2+\alpha}$  increase of the required time resources is deduced for unitary 2D quiet zone acquisitions. These constraints may enforce reduction of the completeness in the acquisition campaigns either in terms of covered number of frequencies, feed-probe configurations or sampling domain extension. In practice, acquisition times are kept reasonable at the expense of shifting from 2D acquisitions towards 1D linear samplings in the main and diagonal cuts.

Our approach here will be not to trade-off the completeness of the probing campaigns but to propose a data reduction scenario which considers the finite SNR figure at millimeter wavelengths with the purpose of reducing dramatically the required number of samples that contribute effectively to the SNR. Seen from a complementary point of view, the degrees of freedom associated to that number of complex samples determine the amount of plane wave spectral modes required to represent the maximum SNR version of the quiet zone fields. For a low-pass nature magnitude, such as the main contribution of the optics, it is equivalent to reach the cutoff frequency of the lowpass filter which maximizes the SNR of a quiet zone distribution. This maximization process might become a mandatory task whenever SNR-sensitive post-processing techniques are applied to the quiet zone information.

This paper is organized as follows: Section 2 proposes a mathematical model of the finite SNR main contribution to the quiet zone fields. Section 3 approaches the quiet zone probing issue proposing a feasible maximal SNR scheme, in practical terms. Section 4 focuses on a useful application of the technique and section 5 draws conclusions as well as future lines.

## 2. Mathematical Model

### 2.1 Noiseless Scenario

In this non bounded dynamic range scenario, the signal of interest is the direct wave contribution to the quiet zone fields  $\mathbf{E}_{QZ}^{(S)}(\mathbf{r})$  within a planar acquisition domain  $\mathbf{r} \in \Omega_A = [x_A^-, x_A^+] \times [y_A^-, y_A^+]$ . The electrical noise contribution is assumed null  $\mathbf{E}_{QZ}^{(N)}(\mathbf{r}) = \mathbf{0}$ .  $\mathbf{E}_{QZ}^{(S)}(\mathbf{r})$  results from the scattering of the reflector's current distribution towards the acquisition plane [4]. Plane wave spectrum approach to  $\mathbf{E}_{QZ}^{(S)}(\mathbf{r})$  [7] proposes its evaluation as the vector integration a of plane waves distribution  $\tilde{\mathbf{E}}(\mathbf{k}_x, \mathbf{k}_y)$  within the visible spectral domain  $\tilde{\Omega}_0 = [-k_0, k_0] \times [-k_0, k_0]$ , of low-pass nature (1). In practice, the set of plane waves which are required to implement the coupling between sources and acquisition plane

$\tilde{\Omega}_{Range} = [-k_{x,max}, k_{x,max}] \times [-k_{y,max}, k_{y,max}]$  is a subset of the

visible domain:  $\tilde{\Omega}_{Range} \subseteq \tilde{\Omega}_0$  [4], [6], whose definition depends on the geometry of the acquisition setup and the physical size of the optics [6]. Thus, no signal is expected on  $\tilde{\mathbf{E}}(\mathbf{k}_x, \mathbf{k}_y)$  for spectral components  $(\mathbf{k}_x, \mathbf{k}_y) \notin \tilde{\Omega}_{Range}$ . According to Fourier theory, a reduction in the extension of a lowpass spectral domain rewrites the Nyquist criterion allowing for larger distances between samples  $\Delta\{x/y\}$  in the transformed (spatial) domain without information losses about the main wave contribution, as in (2).

$$\mathbf{E}_{QZ}^{(ig)}(\mathbf{r}) = \iint_{\tilde{\Omega}_0} \tilde{\mathbf{E}}(\mathbf{k}_x, \mathbf{k}_y) \cdot e^{-j \cdot \mathbf{k} \cdot (\mathbf{r} - \mathbf{r}')} \cdot dk_x \cdot dk_y, \quad (1)$$

$$\Delta\{x/y\} = \frac{\lambda_0}{2} \cdot \frac{k_0}{k_{\{x/y\},max}} \geq \frac{\lambda_0}{2}. \quad (2)$$

Thus, the propagation between the sources' plane  $\Omega_S$  and the acquisition plane  $\Omega_A$  induces a lowpass filtering on the source's spectral distribution  $\tilde{\mathbf{E}}(\mathbf{k}_x, \mathbf{k}_y)$  in addition with a phase weighting  $e^{-j \cdot \mathbf{k} \cdot (\mathbf{r} - \mathbf{r}')}$  which does not affect the spectral contributions' magnitude. The sources' spectral distribution  $\tilde{\mathbf{E}}(\mathbf{k}_x, \mathbf{k}_y)$  follows a diffractive pattern whose envelope decays as following a  $k_{\{x/y\}}^{-1}$  law [8]. In sum, the magnitude of the spectral distribution regarding the noiseless quiet zone  $\tilde{\mathbf{E}}_{QZ}^{(S)}(\mathbf{k}_x, \mathbf{k}_y)$  features a  $k_{\{x/y\}}^{-1}$  decaying pattern within  $\tilde{\Omega}_{Range}$ , being null outside.

$$\begin{aligned} \mathbf{E}_{QZ}^{(S)}(\mathbf{r} \in \Omega_A) &= \iint_{\tilde{\Omega}_{Range}} \tilde{\mathbf{E}}(\mathbf{k}_x, \mathbf{k}_y) \cdot e^{-j \cdot \mathbf{k} \cdot (\mathbf{r} - \mathbf{r}')} \cdot dk_x \cdot dk_y \equiv \dots \\ &\dots \equiv \mathfrak{S}^{+1} \left\{ \tilde{\mathbf{E}}_{QZ}^{(S)}(\mathbf{k}_x, \mathbf{k}_y) \right\} \end{aligned} \quad (3)$$

### 2.2 Finite Dynamic Range Scenario

When the dynamic range available in the setup is finite and potentially low, the measured quiet zone results from the addition of a noise  $\mathbf{E}_{QZ}^{(N)}(\mathbf{r})$  contribution to the signal  $\mathbf{E}_{QZ}^{(S)}(\mathbf{r})$ , as in (3). From the spectral point of view, spectral components  $(\mathbf{k}_x, \mathbf{k}_y) \in \tilde{\Omega}_{Range}$  may have a stronger contribution of noise than signal:  $\|\tilde{\mathbf{E}}_{QZ}^{(N)}(\mathbf{k}_x, \mathbf{k}_y)\| > \|\tilde{\mathbf{E}}_{QZ}^{(S)}(\mathbf{k}_x, \mathbf{k}_y)\|$ . The consequence is SNR degradation in the measured quiet zone distribution. In this scenario with a finite dynamic range,  $\tilde{\mathbf{E}}_{Meas}(\mathbf{k}_x, \mathbf{k}_y)$  can thus be modeled as the addition of the signal of interest  $\tilde{\mathbf{E}}_{Acq}^{(S)}(\mathbf{k}_x, \mathbf{k}_y)$  plus an uncorrelated noise contribution  $\tilde{\mathbf{E}}_{Acq}^{(N)}(\mathbf{k}_x, \mathbf{k}_y)$ , as in (4). The magnitude of this noise  $\sqrt{\sigma_{Acq}^{(N)}}$  satisfies (5) and (6), where  $dr$  is the dynamic range

offered by the setup, in natural units. Fig. 1 depicts a scenario for which  $\tilde{\mathbf{E}}_{QZ}^{(S)}$  is nonzero for  $k_{\{x/y\}} \leq 0.3k_0$ .

$$\tilde{\mathbf{E}}_{Meas}(k_x, k_y) = \tilde{\mathbf{E}}_{QZ}^{(S)}(k_x, k_y) + \tilde{\mathbf{E}}_{QZ}^{(N)}(k_x, k_y), \quad (4)$$

$$\|\tilde{\mathbf{E}}_{QZ}^{(N)}(k_x, k_y)\| = \sqrt{\sigma^{(N)}} \cdot N_0^l(k_x, k_y), \quad (5)$$

$$\sqrt{\sigma^{(N)}} = \frac{\tilde{\mathbf{E}}_{QZ}^{(S)}(\mathbf{k} = \mathbf{0})}{dr}. \quad (6)$$

Thus, it is relevant to define a maximally compact spectral support  $\tilde{\Omega}_{SNR} = [-k_{SNR,x}, k_{SNR,x}] \times [-k_{SNR,y}, k_{SNR,y}]$  that ensures positive SNR in addition with the least severe loss of information, as in (7). It can be demonstrated that  $\tilde{\Omega}_{SNR}$  converges to  $\tilde{\Omega}_{Range}$  in an infinite dynamic range, noiseless scenario. The considered spectral domains satisfy (8).

$$\|\tilde{\mathbf{E}}_{QZ}^{(N)}(k_x, k_y)\| > \|\tilde{\mathbf{E}}_{QZ}^{(S)}(k_x, k_y)\| \quad \forall \mathbf{k} \notin \tilde{\Omega}_{SNR}, \quad (7)$$

$$\tilde{\Omega}_{SNR} \subseteq \tilde{\Omega}_{Range} \subseteq \tilde{\Omega}_0. \quad (8)$$

The boundaries of  $\tilde{\Omega}_{SNR}$  are  $k_x = k_{SNR,x}$ ,  $k_y = k_{SNR,y}$  and can be approached either theoretically or experimentally. In the first case, some assumptions should be taken about the source's distribution  $\mathbf{M}(\mathbf{r}')$  and reach a heuristic version of  $\tilde{\mathbf{E}}_{QZ}^{(S)}(k_x, k_y)$ . For an ideal scheme,  $\mathbf{M}(\mathbf{r}')$  converges to a phase uniform, magnitude tapered distribution within the effective sources extension  $\Omega_S^{eff} \subset \Omega_S$ , potentially the main reflector's non-serrated area. The serrations taper  $\mathbf{M}(\mathbf{r}')$  towards  $\mathbf{0}$ . This sources distribution generates a diffractive low pass [9] pattern  $\tilde{\mathbf{E}}_{Acq}^{(S)}(k_x, k_y)$  for which the non-oscillating envelope decays following a  $k_{\{x/y\}}^{-1}$  law [8]. Being  $k_{SNR,\{x/y\}}^*$  the heuristic approach to  $k_{SNR,\{x/y\}}$ , it can be analytically deduced as in (9), which is used to draw the plot in Fig. 2, representing  $k_{SNR,\{x/y\}}^*$  as a function of the available dynamic range and frequency of operation.  $k_{SNR,\{x/y\}}^*$  must be seen as the lower bound for  $k_{SNR,\{x/y\}}$  (10), given that it works under the assumption of ideal collimation scheme. In an experimental deduction of  $k_{SNR,\{x/y\}}$ , a two mid-resolution cuts in the horizontal and vertical dimensions should be performed to have a realistic image of the behavior in  $\tilde{\mathbf{E}}_{Acq}(k_x, k_y)$ , and thus know for which spectral components the SNR is positive. Both in the experimental and the theoretical approaches, the available dynamic range can be extracted from a time-domain plot of the  $|S_{2,1}(\mathbf{t})|$  coupling between feed and probe along a radar distance which is able to cover the direct wave timeslot as well as time periods where no signal (either direct or stray) is expected

$$\frac{2}{\pi |X_S^+ - X_S^-|} \cdot \left(k_{SNR,\{x/y\}}^*\right)^{-1} - dr = 0, \quad (9)$$

$$k_{SNR,\{x/y\}}^* \leq k_{SNR,\{x/y\}}. \quad (10)$$

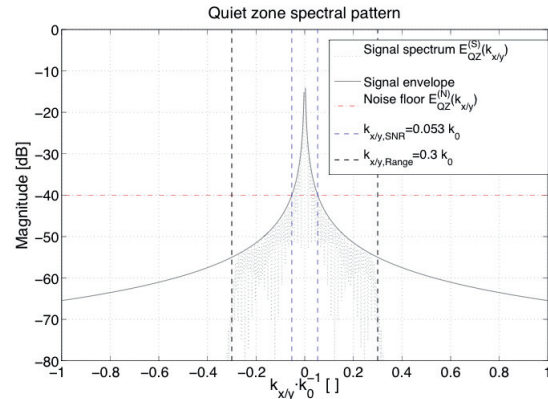


Fig. 1. Spectral distribution of a low dynamic range quiet zone acquisition.

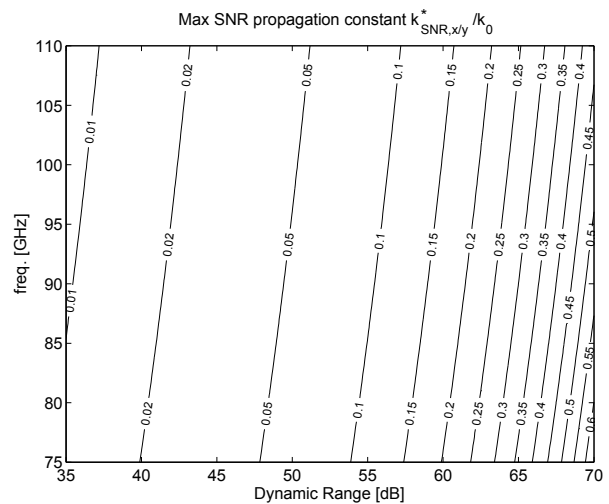


Fig. 2. Theoretical approach to  $k_{SNR,\{x/y\}}^*$ .

### 3. Probing Setup: Implementation

In this section, it is proposed a Cartesian grid probing technique which implements the SNR maximization approach to the quiet zone fields. The sampling must satisfy (9) proposing a maximally compact  $\tilde{\Omega}_{SNR}$  domain. According to Fourier theory, the sampling distances  $\Delta\{x/y\}_a$  for in the acquisition plane would satisfy (11). Being  $\Omega_A = [x_A^-, x_A^+] \times [y_A^-, y_A^+]$  the acquisition domain, the required number of samples in the x/y direction  $N\{x/y\}_a$  follows (12).

$$\Delta\{x/y\}_a = \frac{\pi}{k_{SNR,\{x/y\}}^*} = \pi \cdot dr^{-1} \quad (11)$$

$$N\{x/y\}_a = 1 + \left( \{x/y\}_a^+ - \{x/y\}_a^- \right) \cdot \pi^{-2} \cdot dr. \quad (12)$$

The SNR increase in natural magnitude with respect to the most general version of the Nyquist sampling approach is the fraction between: the SNR achieved by the proposed technique, divided by the SNR figure drawn by Nyquist, as in (13). Equation (13) becomes (14) when the definition of  $\tilde{\Omega}_{SNR}$  fulfills the sampling approach of (11). The corresponding SNR increase in dB follows (15).

$$\begin{aligned} \Delta_{SNR} &= \frac{\left[ \int_{\tilde{\Omega}_{SNR}} \|\tilde{\mathbf{E}}_{QZ}^{(S)}(k_x, k_y)\|^2 \cdot dk_x \cdot dk_y \right] / \int_{\tilde{\Omega}_{SNR}} dr^{-2} \cdot dk_x \cdot dk_y}{\left[ \int_{\tilde{\Omega}_0} \|\tilde{\mathbf{E}}_{QZ}^{(S)}(k_x, k_y)\|^2 \cdot dk_x \cdot dk_y \right] / \int_{\tilde{\Omega}_0} dr^{-2} \cdot dk_x \cdot dk_y} = \dots \\ &= \frac{\left[ \int_{\tilde{\Omega}_{SNR}} \|\tilde{\mathbf{E}}_{QZ}^{(S)}(k_x, k_y)\|^2 \cdot dk_x \cdot dk_y \right]}{\left[ \int_{\tilde{\Omega}_0} \|\tilde{\mathbf{E}}_{QZ}^{(S)}(k_x, k_y)\|^2 \cdot dk_x \cdot dk_y \right]} \cdot \frac{k_0^2}{k_{SNR,x} \cdot k_{SNR,y}} \end{aligned} \quad (13)$$

$$\Delta_{SNR} = \frac{\left[ \int_{\tilde{\Omega}_{SNR}} \|\tilde{\mathbf{E}}_{QZ}^{(S)}(k_x, k_y)\|^2 \cdot dk_x \cdot dk_y \right]}{\left[ \int_{\tilde{\Omega}_0} \|\tilde{\mathbf{E}}_{QZ}^{(S)}(k_x, k_y)\|^2 \cdot dk_x \cdot dk_y \right]} \cdot \frac{4 \cdot \pi^2 \cdot dr^{-2}}{\lambda_0^2} \geq 1 \quad (14)$$

$$\Delta_{SNR} = 10 \cdot \log_{10}(\Delta_{SNR}) \geq 0. \quad (15)$$

A priori knowledge of the  $\tilde{\mathbf{E}}_{QZ}^{(S)}(k_x, k_y)$  pattern would lead to an optimal  $\tilde{\Omega}_{SNR}$  which reaches the maximum  $\Delta_{SNR}$ . At this point, the collimated phase hypothesis is not able to contribute to this task, given that it is too simplifying to be considered to integrate the spectral contributions of  $\tilde{\mathbf{E}}_{QZ}^{(S)}(k_x, k_y)$  within a certain domain.

### 4. Application

After performing a 2D acquisition of the quiet zone, probe correction techniques are of interest in order to remove the contribution of the probe antenna over the results. For the planar case [10], the probe correction consists on weighting the acquired spectrum  $\tilde{\mathbf{E}}_{Acq}(k_x, k_y)$  through the inverse of the probe's plane wave spectrum tensor  $\mathbf{R}(k_x, k_y)$  (16). This matrix can be expressed as a function of the probe's co-polar  $r_{VV}(k_x, k_y)$  and cross-polar distributions  $r_{HV}(k_x, k_y)$ , as in (17).

$$\begin{bmatrix} \tilde{E}_x(k_x, k_y) \\ \tilde{E}_y(k_x, k_y) \end{bmatrix}_{Acq} = \mathbf{R}(k_x, k_y) \begin{bmatrix} \tilde{E}_x(k_x, k_y) \\ \tilde{E}_y(k_x, k_y) \end{bmatrix}_{QZ} \quad (16)$$

$$\begin{aligned} \mathbf{R}(k_x, k_y) &= \begin{bmatrix} r_{HH}(k_x, k_y) & r_{VH}(k_x, k_y) \\ r_{HV}(k_x, k_y) & r_{VV}(k_x, k_y) \end{bmatrix} \\ &= \begin{bmatrix} r_{VV}(-k_y, k_x) & r_{HV}(-k_y, k_x) \\ r_{HV}(k_x, k_y) & r_{VV}(k_x, k_y) \end{bmatrix} \end{aligned} \quad (17)$$

For low cross-pol probes,  $\mathbf{R}^{-1}(k_x, k_y)$  simplifies as (18). This can be used to perform a full vector characterization of the different feed-probe configurations, as in (19), (20).

$$\mathbf{R}^{-1}(k_x, k_y) = \begin{bmatrix} 1/r_{VV}(-k_y, k_x) & 0 \\ 0 & 1/r_{VV}(k_x, k_y) \end{bmatrix} \quad (18)$$

$$\begin{bmatrix} \tilde{E}_{HH}(k_x, k_y) \\ \tilde{E}_{VV}(k_x, k_y) \end{bmatrix}_{QZ} = \mathbf{R}^{-1}(k_x, k_y) \begin{bmatrix} \tilde{E}_{HH}(k_x, k_y) \\ \tilde{E}_{VV}(k_x, k_y) \end{bmatrix}_{Acq} \quad (19)$$

$$\begin{bmatrix} \tilde{E}_{VH}(k_x, k_y) \\ \tilde{E}_{HV}(k_x, k_y) \end{bmatrix}_{QZ} = \mathbf{R}^{-1}(k_x, k_y) \begin{bmatrix} \tilde{E}_{VH}(k_x, k_y) \\ \tilde{E}_{HV}(k_x, k_y) \end{bmatrix}_{Acq} \quad (20)$$

The  $\mathbf{R}^{-1}(k_x, k_y)$  inversion is mathematically possible whenever  $r_{VV}(k_x, k_y)$  does not contain nulls for the spectral components to be compensated. The physical implication is that acquisitions performed with certain probes might not be probe compensable, if that is the case. Besides this constraint, the  $1/r_{VV}(k_x, k_y)$  coefficient is, in most cases, expected to increase when  $(k_x, k_y)$  directions move away from boresight. The consequence is SNR decrease, given that the spectral weighting  $\mathbf{R}^{-1}(k_x, k_y)$  reduces the ratio between the direct ray signal  $\tilde{\mathbf{E}}_{QZ}^{(S)}(k_x, k_y)|_{(k_x, k_y) \rightarrow \mathbf{0}}$  and these noisy components

$$\left\{ \left\| \tilde{\mathbf{E}}_{QZ}^{(N)}(k_x, k_y) \right\| > \left\| \tilde{\mathbf{E}}_{QZ}^{(S)}(k_x, k_y) \right\| \right\}_{(k_x, k_y) \rightarrow (k_{x,max}, k_{y,max})}$$

Thus, the proposed technique contributes this evidence offering a maximum SNR figure for the acquired data making it more robust to noise *ab initio* and accordingly increasing the SNR of the post-processed data.

### 5. Conclusions – Future Work

A simple quiet zone probing technique has been proposed in this paper, being its interest emerging from evident bottlenecks at millimeter wavelength frequencies. Mathematical description has been proposed for CATR facilities, based on nearfield theory and analytical formulations have been given to make it applicable to an arbitrary setup. Finally, notes have been given for a potential application for which the SNR increase becomes a critical aspect. Future work consists on the employment of this technique in a real setup so empirical information is obtained about its performance.

## Acknowledgements

The first author wishes to thank the former Spanish Ministry of Science and Innovation for the support provided through the *FPI* scholarship, which funded the research work described in this paper.

## References

- [1] OLVER, A. D. Compact antenna test ranges. In *Seventh International Conference on Antennas and Propagation ICAP 91*. 15-18 Apr 1991, vol. 1, p. 99-108.
- [2] VAN SOMEREN GREVE, S. C., VAN DE COEVERING, L. G. T., VOKURKA, V. J. On design aspects of compact antenna test ranges for operation below 1 GHz. In *Proc. Antenna Measurement Techniques Association Symposium*. Monterey Bay (CA), 1999, p. 248-253.
- [3] JENSEN, F., HEIGHWOOD NIELSEN, P., SALGHETTI DRIOLI, L., PAQUAY, M. Best-Fit Adjustment on the reflectors in a compact range. In *Proc. Antenna Measurement Techniques Association Symposium*. Salt Lake City (USA), 2009.
- [4] MUÑOZ-ACEVEDO, A., SIERRA-CASTANER, M. An efficient hybrid GO-PWS algorithm to analyze conformal serrated-edge reflectors for millimeter-wave compact range. *IEEE Transactions on Antennas and Propagation*, 2012, vol. 60, no. 2, p.1192-1197.
- [5] SALGHETTI, L., PAQUAY, M., ALLART, X. How large is your quiet zone? In *Proc. Antenna Measurement Techniques Association Symposium*. Atlanta (USA), 2010.
- [6] MUÑOZ-ACEVEDO, A., ROLO, L., PAQUAY, M., SIERRA-CASTAÑER, M. Accurate and time efficient quiet zone acquisition technique for the assessment of ESA's CATR at millimeter wavelengths. In *Proc. Antenna Measurement Techniques Association Symposium*. Englewood, October 16-21 2011.
- [7] CLEMMOW, P. A. *The Plane Wave Spectrum Representation of Electromagnetic Fields*. New Jersey: IEEE Press, reissued edition 1996.
- [8] OPPENHEIM, A. V., SCHAFER, R. W. *Discrete Time Signal Processing*, Ed. Prentice-Hall 1997.
- [9] JOY, E., PARIS, D. Spatial sampling and filtering in near-field measurements. *IEEE Transactions on Antennas and Propagation*, May 1972, vol. 20, no. 3, p. 253- 261.
- [10] YAGHJIAN, A. An overview of near-field antenna measurements. *IEEE Transactions on Antennas and Propagation*, Jan 1986, vol. 34, no. 1, p. 30- 45.

## About Authors

**Alfonso MUÑOZ-ACEVEDO** (S'09) was born in Toledo, Spain, in 1985. He received an Engineer of Telecommunication degree in 2008 from the Technical University of Madrid, Spain. Since September 2007, he has been with the Radiation Group of the Technical University of Madrid, as PhD candidate. In summer 2009, he carried out a PhD short stay at the Department of Radio Science and Engineering, Helsinki University of Technology. During 2011, he carried out a stay on millimeter wavelength quiet zone characterization and assessment at the Antennas and Sub/millimetre Waves Section of the European Space Research and Technology Centre ESA-ESTEC located at Noordwijk, The Netherlands. His research interests focus on transversal studies on millimeter wavelength - CATR facilities, from EM analysis towards range assessment and compensation. In 2009 Mr. Muñoz-Acevedo received the National Spanish Board of Electrical Engineers Award to the best Master Thesis of the year on Electrical Engineering.

**Manuel SIERRA-CASTAÑER** (S'95 - M'01) was born in Zaragoza (Spain) in 1970. He obtained the degree of Telecommunication Engineering in 1994 and the PhD in 2000, both from the Technical University of Madrid (UPM) in Spain. He worked for the cellular company Airtel from 1995 to 1997. Since 1997, he worked in the University "Alfonso X" as assistant, and since 1998 at the Technical University of Madrid as research assistant, assistant and associate professor. He is member of the IEEE. His current research interests are in planar antennas and antenna measurement systems. In 2007 Dr. Sierra-Castañer obtained the IEEE APS 2007 Schelkunoff Prize paper Award for the paper "Dual-Polarization Dual-Coverage Reflectarray for Space Applications".